Productive infection of double-negative T cells with HIV *in vivo*

Gilles Marodon*, David Warren, Michael C. Filomio, and David N. Posnett†

Department of Medicine, Division of Hematology/Oncology, Cornell University, Joan and Sanford I. Weill Medical College, New York, NY 10021

Edited by Anthony S. Fauci, National Institutes of Health, Bethesda, MD, and approved August 3, 1999 (received for review, June 1, 1999)

HIV induces CD4 down-regulation from the surface of infected cells by several independent mechanisms, suggesting an important biological role for this phenomenon. *In vitro* CD4 down-regulation generates T cells with a double-negative (DN) $CD4^-CD8^-$ T cell receptor-$\alpha\beta^+$ phenotype. However, evidence that this down-regulation occurs *in vivo* in HIV-infected subjects is lacking, and viral load or viral production assays invariably focus on $CD4^+$ T cells. We show here that HIV infection can often be detected in sorted DN cells from peripheral blood and lymph nodes, even when plasma viral load is undetectable. DN T cells infected with HIV represented up to 20% of the cellular viral load in T cells, as determined by DNA PCR. In patients on successful highly active antiretroviral therapy, the viral load decreased in the plasma in $CD4^+$ and in DN T cells, suggesting that infected DN cells, like $CD4^+$ cells, contribute to viral production and are sensitive to highly active antiretroviral therapy. Indeed, HIV unspliced and multispliced RNAs were often detectable in DN T cells in spite of the small size of this subset. Infectious virus from DN T cells was transmitted efficiently in coculture experiments with uninfected T cell lymphoblasts, even when viral DNA in the DN cells was barely detectable. We conclude that a discrete population of infected DN T cells exists in HIV-positive subjects, even when the plasma viral load is undetectable. These cells may represent an important source of infectious virus.

Like other retroviruses, HIV down-regulates its own receptor (1, 2). CD4 down-regulation may alter signaling pathways because of the association of CD4 with $p56^{lck}$ (3), protect from glycoprotein (gp120)-induced apoptosis (4), or prevent superinfection (5). However, evidence for CD4 down-regulation in HIV-positive subjects is still lacking and most prior work was performed with transformed cell lines with unknown relevance *in vivo*. CD4 down-regulation occurs in primary human peripheral blood lymphocytes (PBL) infected with a reporter virus (6, 7). For example, in PBL infected with HIV-HSA (HIV with a murine heat stable antigen reporter gene), HSA^+ cells progressively lost CD4 expression, while maintaining high levels of CD4 mRNA and unaltered levels of T cell receptor (TCR) and CD8 expression (7). Therefore, infected double-negative (DN) T cells are generated from $CD4^+$ precursors. In normal subjects, DN cells are a heterogeneous population. They include natural killer T cells implicated in initiation of a T helper-2 response (8). Whether such normal DN subsets can become HIV infected is not known.

In earlier *ex vivo* studies, HIV DNA seemed to be exclusively in the $CD4^+$ population of peripheral T lymphocytes (9, 10). We now know that $CD8^+$ cells can also be infected (11, 12), but there are no data on DN T cells obtained *ex vivo*.

This paper examines the prevalence of detectable HIV DNA and HIV-encoded RNAs in DN cells and the ability of DN cells to produce infectious virus in a coculture assay. We show that infected DN cells are often detectable in patients on successful highly active antiretroviral therapy (HAART). Thus, these cells may be important in promoting persistence of long-term infection.

Methods

Human Subjects. Informed consent was obtained from patients at various New York Hospital clinics. The clinical parameters given in Table 1 are those at the time of study, unless indicated otherwise. Patients were placed in two groups as defined by response to HAART (see Table 1). Significance was determined by *t* test. A separate nonoverlapping cohort of patients was examined (see Fig. 4 and Table 2).

Cell-Sorting Strategy and Efficiency. PBL were isolated on Ficoll/Hypaque (Amersham Pharmacia) and stained with optimal dilutions of anti-CD4-biotin (clone FFB2.3), anti-TCR-$\alpha\beta$-FITC (T10B9, PharMingen), and anti-CD8-phycoerythrin (HIT8α, PharMingen). Cells were incubated for 20 min at 4°C with CD4-biotinylated antibody, washed with PBS/10% (vol/vol) FBS/0.01% sodium azide, incubated with anti-TCR-FITC antibody, washed again, incubated with Streptavidin-Tricolor (Caltag, South San Francisco, CA) and CD8-phycoerythrin antibody, and finally fixed in 1% paraformaldehyde. Gates were set as indicated in Fig. 1 for sorting with a fluorescence-activated cell sorter. (FACSvantage, Becton Dickinson).

HIV *gag* DNA PCR. DNA was prepared by lysing cell pellets in 0.1 M Tris·Cl/10 mM EDTA/600 μg/ml proteinase K at 56°C for 1 h followed by 95°C for 15 min. DNA (10 μl) was used in a 50-μl PCR containing 12.5 pmol primers, 10 mM Tris·HCl, 50 mM KCl, 0.01% gelatin, 0.1% Triton X-100, 0.1 mM dNTPs, 1 unit *Taq* polymerase, 3 mM $MgCl_2$ (Promega), and 2.5 μCi of [α-^{32}P]dCTP (Amersham Pharmacia). Primers SK38 and SK39 (13) were used to detect *gag*. Primers DQ28 and DQ29 amplify cellular HLA-DQα and were used to quantify total cellular DNA (14). PCR conditions for *gag* were 1 cycle at 94°C for 3 min; followed by 28 cycles at 94°C for 30 s, 60°C for 30 s, and 72°C for 30 s; with a final extension cycle at 72°C for 10 min. At 28 cycles, the PCR had not yet reached saturation as determined in preliminary experiments with different numbers of cycles. Portions (10 μl) of each PCR were run on an 8% acrylamide gel. Gels were exposed to a Phosphoscreen detector (Molecular Dynamics) and scanned on a STORM PhosphorImager (Molecular Dynamics). Band intensities were measured by using SCANDNASIS (Hitachi Software, Tokyo).

HIV *gag* Copy Numbers per Subset. A standard linear curve for the HIV *gag* PCR was obtained by using 10- and 5-fold dilutions of the ACH-2 cell line containing a single copy of the HIV genome. Linear equations of these curves were used to estimate HIV copy numbers for each sample. This estimate was corrected by cell numbers from the FACSvantage counters after sorting. Reproducibility of these estimates is shown for Met90, where similar values were obtained from two separate sorts (Fig. 2*B*). The correlation between the intensity of PCR bands for cellular DQ DNA and cell counts after sorting ($r = 0.83$) was calculated by

This paper was submitted directly (Track II) to the PNAS office.

Abbreviations: gp, glycoprotein; DN, double negative; TN, triple negative; HAART, highly active antiretroviral therapy; PBL, peripheral blood lymphocyte; MS, multispliced; US, unspliced; TCR, T cell receptor; FACS, fluorescence-activated cell sorter; LN, lymph nodes; RT-PCR, reverse transcription–PCR.

*Present address: Centre National de la Recherche Scientifique-ESA 7087, Bât CERVI, 83 Boulevard de l'Hôpital, 75651 Paris Cedex 13, France.

†To whom reprint requests should be addressed. E-mail: dposnett@mail.med.cornell.edu.

The publication costs of this article were defrayed in part by page charge payment. This article must therefore be hereby marked "*advertisement*" in accordance with 18 U.S.C. §1734 solely to indicate this fact.

Table 1. Clinical characteristics of patients

HIV DNA in cell type	Patients*	Age, years	Gender†	CD4 count per mm³	Viral load, copies per ml‡	Present medications§				Duration of present treatment, months (or year of diagnosis)	Response to HAART¶
						PI	NRT	NNRT	Other		
CD4	CSS9	44	M	257	<400	1	1	1	—	4	+
	CSS12	37	M	522	<400	1	2	—	—	7	+
	H1	41	M	659	4,266	—	—	—	—	Naive (1985)	NA
	Met91	43	F	268	36,349	—	—	—	—	Naive (1990)	NA
CD4 DN	CSS22	33	M	241	632	1	2	1	—	6	+
	CSS25	37	F	265	1,318	1	2	1	—	3	+
	CSS21	36	M	437	<400	1	2	—	—	22	+
	CSS8.1	44	M	717	546	—	3	—	—	8	+
	CSS8.2	—	—	595	<400	—	3	1	—	6	+
	CSS10	34	F	337	<400	1	2	—	—	11	+
	CSS15	53	M	469	18,109	1	2	—	—	1	+
	CSS13	39	M	92	<500	1	2	—	—	7	+
	CSS23	44	M	287	<25	1	2	—	T	18	+
	CSS26	25	T	96	198,996	—	—	—	—	Naive (1995)	NA
	Met70	44	M	354	15,930	1	2	—	—	6	−
	Met90.1	39	M	253	64,000	1	1	—	T	1	−
	Met90.2	—	—	195	53,000	1	1	—	T	2	−
	Met90.3	—	—	220	<400	1	2	1	T	7	+
CD4 DN CD8	CSS19	47	M	518	157,000	—	—	—	ZI	1	−
	CSS20	38	M	141	121,292	—	—	—	—	—	−
	CSS24	39	T	303	>1,000,000	—	1	1	—	2	−
	CSS3	47	M	146	100,479	—	—	—	—	—	−
	CSS18	36	F	965/363	<400/233,272	1	3	—	—	5	NA
	CSS16.1	45	M	388	9,000	—	—	—	—	Naive (1991)	NA
	CSS16.2	—	—	566	11,498	—	—	—	—	—	NA

Patients are arranged in three groups: HIV detectable (*i*) in only CD4, (*ii*) in CD4 and DN, and (*iii*) in CD4, DN and CD8. For CSS23 (see below), one experiment (shown in Fig 2*A*) revealed HIV DNA only in DN cells, but in another experiment, HIV DNA was also found in CD4 T cells.

*CSS denotes patients from an AIDS clinic at New York Hospital (NYH); Met denotes a methadone maintenance clinic at NYH; and H denotes a hemophilia clinic at NYH.

†M, male; F, female; T, transgender (genetic male on female hormones).

‡Viral copies per ml were assessed by RNA PCR (Roche Diagnostics), or by bDNA assay (Chiron) in CSS13 and CSS23. When two values are indicated (CSS18), the experimental sample was obtained within a few months in between.

§The number of HAART medicines within each class of drugs is indicated. PI, protease inhibitors (Crixivan, indinavir; Viracept, nelfinavir; Invirase, saquinavir); NRT, nucleoside RT inhibitors (Zidovine, AZT; Zerit, D4T; Epivir, 3TC; Hivid, DDC; Videx, DDI); NNRT, nonnucleoside RT inhibitors (Viramune, nevirapine; Rescriptor, dilavridine); and other (T, interleukin-2; ZI, Zintevir, AR177, an integrase inhibitor).

¶Response to HAART is defined as >70% decrease in the viral load or consistently undetectable viral load. NA, not applicable.

using a simple curve fit with CRICKET GRAPH 1.3 (Cricket Software, Malvern, PA).

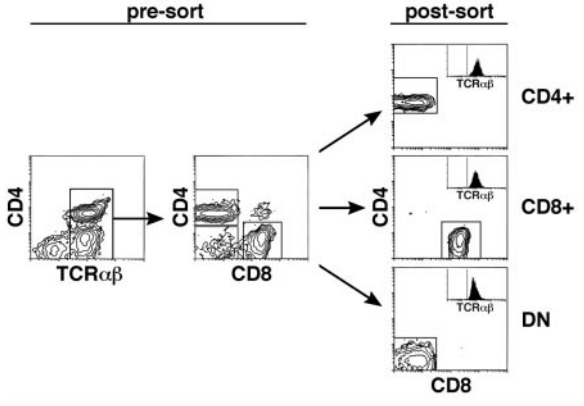

Fig. 1. Cell-sorting strategy and efficiency. Presort gates were set around TCR$^+$ cells. Subsequently, CD4$^+$CD8$^-$, CD4$^-$CD8$^-$, and CD4$^-$CD8$^+$ cells were sorted. Typically, the purity for the sorted T cells subsets exceeded 98%, and the sorted subsets were virtually all TCR-$\alpha\beta^+$ (*Insets*).

Magnetic Bead Sorting. PBL were first incubated with a mouse anti-human CD4 antibody (FFB2.3) for 1 h at 4°C. CD4$^+$ cells were positively selected with magnetic beads coated with a goat anti-mouse antibody as recommended by the manufacturer (Dynal, Great Neck, NY). The same procedure was repeated sequentially for CD8$^+$ and CD3$^+$ cells to get the CD3$^+$ DN. Note that for some data (see Table 2 and Fig. 4), the CD4 and CD8 antibodies were used simultaneously to isolate a common subset including CD4 single positives, CD8 single positives, and possible CD4/8 double positives (CD4 + CD8). The efficacy of the sorts was >95%. The triple-negative (TN) fraction (CD4$^-$CD8$^-$CD3$^-$), i.e., the remaining negatively sorted cells, contained B cells, monocytes, and natural killer cells (data not shown) and served as an internal control.

HIV RNA in T Cell Subsets. RNA was isolated, and cDNA was synthesized (7). cDNA was diluted to obtain substrate cDNA levels corresponding to the indicated cell number equivalents. PCR with primers specific for MS, US, and actin RNA were performed (ref. 7; see Table 2 and Fig. 4).

Coculture Infectivity Assay. The different fractions of cells complexed with magnetic beads were plated directly with 2×10^6 to 3×10^6 phytohemagglutinin-activated blasts (harvested after 2

IMMUNOLOGY

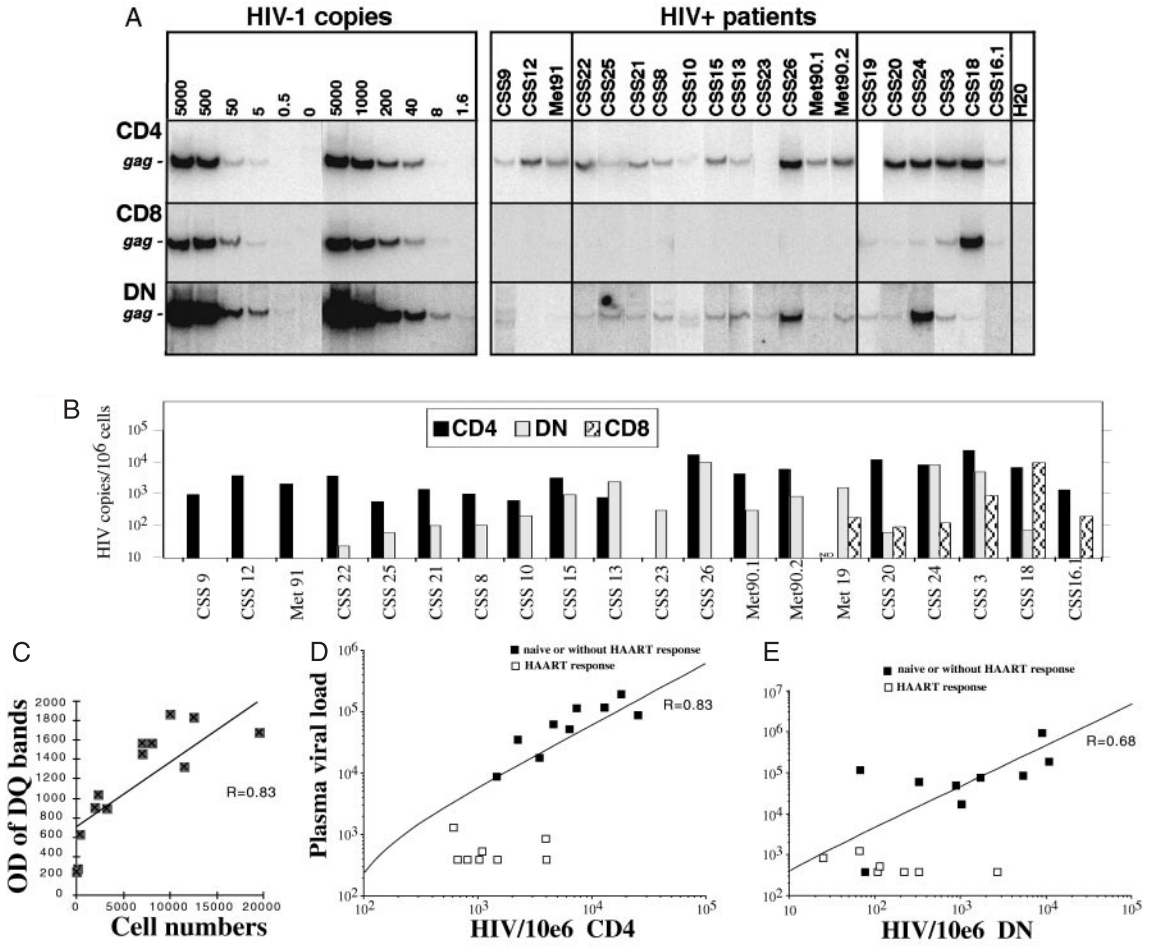

Fig. 2. (*A*) HIV *gag* DNA PCR in sorted subsets from 19 HIV-infected individuals. Gels were exposed to a Phosphoscreen detector (Molecular Dynamics) and scanned on a PhosphorImager. The controls, labeled HIV-1 copies, represent the indicated cell numbers of ACH-2 cells, containing a single copy of HIV-1 per cell, that were diluted in a constant number of uninfected CEM cells (14). The patient samples are arranged in the same order in Table 1. (*B*) Estimate of HIV *gag* copy numbers in each sorted cell subset and quantification of the band intensities (see *A*). The estimated *gag* copy numbers were corrected by cell numbers, as measured with the FACSvantage counters at the end of each sort. (*C*) Correlation between cell number equivalents used for PCR and intensity of HLA-DQα PCR bands. Band intensities of cellular DQα PCRs correlated well with cell number equivalents determined by the FACS counter at the end of each sort. A good correlation was obtained with samples derived from sorted DN subsets of HIV-positive patients (similar results were obtained with sorted CD4 subsets). This result rules out variable efficiencies of DNA isolation and PCR amplification and indicates that the chosen range of cell number equivalents (<20,000 DN cells) allows quantitative assessment of cellular DNAs, such as HLA DQα. It also shows that HIV *gag* copy number can be calculated as a function of cell number (see *B*). (*D*) The correlation between plasma viral load and CD4 cellular viral load indicates that there is a variable viral load in CD4 cells in HAART-treated patients who have no detectable plasma viral load. (*E*) The correlation between plasma viral load and DN cellular viral load indicates that there is a variable viral load in DN T cells in HAART-treated patients who have no detectable plasma viral load. Undetectable plasma viral loads were assigned a value of 400 RNA copies per ml, i.e., the limit of detection of the clinical test used.

days) from a noninfected individual and cultured in the presence of IL-2 for 2–4 weeks. Cell-free supernatants were collected every 3–4 days and stored at −20°C. p24 was measured in the supernatants by using an ELISA kit (NEN).

Results

To test whether HIV-infected DN T cells exist *in vivo*, peripheral blood T cells from 19 HIV-infected individuals (Table 1) were sorted based on expression of TCR$\alpha\beta$, CD4, and CD8 (Fig. 1). DNA from the sorted subsets was analyzed by PCR (Fig. 2*A*). HIV *gag* DNA was detected in CD4$^+$ T cells from 94% (17 of 18) of the HIV-positive individuals studied. HIV was found in DN T cells from 84% (16 of 19) of these individuals. The high frequency of HIV detection in DN cells was confirmed by using primers specific for the *pol* gene of HIV (data not shown). By contrast, HIV *gag* was detected in the CD8$^+$ fraction in only 31% (6 of 19) of HIV-positive individuals. The number of viral copies per million cells was then estimated (Fig. 2*B*). The cell number equivalents used for PCR correlated well with PhosphorImager band intensity of HLA-DQ PCR bands, as a measure of consistent PCR efficiency (Fig. 2*C*). Therefore, we used cell number data to calculate viral loads per 10^6 cells (Fig. 2*B*).

The numbers of viral copies were 5,146 ± 6,591 *gag* copies per 10^6 cells (mean ± SD; range undetectable to 17,937) in the CD4$^+$ subset and 1,603 ± 3,047 *gag* copies per 10^6 cells (range undetectable to 10,564) in the DN subset. The highest viral copy numbers in the DN subset were detected in subjects CSS3, CSS13, CSS19, CSS24, and CSS26. Of these patients, four had high plasma viral loads, and one (CSS13) had undetectable plasma viral loads. HIV-positive DN T cells were often present in subjects without detectable plasma viral load after successful HAART. Among the seven HIV-positive subjects with undetectable plasma viral loads (Table 1), five had HIV DNA in the DN subset, whereas all had HIV DNA in CD4$^+$ and none had HIV DNA in CD8 cells. In most patients, the DNA viral load was higher in CD4 versus DN cells, but in some patients (CSS13, CSS24, and CSS26) the viral loads per 10^6 cells were about equivalent for CD4 and DN T cells. Considering, on average, 5- to 10-fold greater numbers of CD4 than DN T cells, the viral load in the DN subset represented 10–20% of the total T cell

viral DNA in these patients. We conclude that a significant number of HIV-infected T cells have a DN phenotype.

The number of viral copies in the $CD8^+$ subset was 589 ± 2,276 *gag* copies per 10^6 cells (range undetectable to 10,220). However, data from a single patient (CSS18) contributed heavily to this average. In contrast to a previous study (11), HIV-infected $CD8^+$ cells were not detected frequently, perhaps because we used a 28-cycle PCR, which is more stringent than the 45-cycle PCR used in the previous study.

Plasma viral loads were correlated with cellular viral loads in CD4 and DN T cells in patients with or without HAART (Fig. 2 *D* and *E*). Among patients that were treatment naive or had failed HAART, there was a strict correlation between plasma and cellular viral loads. Among patients with a HAART response (see Table 1), plasma viral loads generally were undetectable, but cellular viral loads were variably present in both CD4 and DN T cells. However, the average CD4 and DN viral loads were decreased by about one log in patients with a HAART response (Fig. 2 *D* and *E*). Therefore, successful HAART resulted in decreases of both cellular viral loads and plasma viral load. This result implied that HIV-infection in DN T cells was sensitive to antiviral therapy and therefore was likely a productive infection, as opposed to infection with defective virus.

Lymph nodes (LN) are thought to represent a major source of viral production and a site of entrapment of plasma virions (15, 16). Teased LN cells were sorted as described in Fig. 1. HIV *gag* DNA was detected in $CD4^+$ and in DN T cells from two HIV-infected LN (Fig. 3*A*). In LN1141, viral copy numbers were similar in $CD4^+$ and DN subsets (Fig. 3*B*). By contrast, in LN791, HIV DNA was infrequent in DN T cells (Fig. 3*B*). MS RNA was present in $CD4^+$ and DN T cells from LN1141, indicating productive infection of both subsets. MS RNA was barely detectable in $CD4^+$ and undetectable in DN cells of LN791, indicating lower levels of productive infection in LN791 (Fig. 3*A*). In this instance, low levels of productive infection correlated with lower levels of HIV *gag* DNA in the DN subset but had no apparent effect on the levels of HIV *gag* in the $CD4^+$ subset. Thus, the level of HIV DNA in the DN subsets may perhaps serve as a surrogate indicator of productive infection.

To test further whether infection of DN T cells was productive, we examined HIV MS RNA, US RNA, and cellular actin RNA in fresh *ex vivo* PBL samples from 10 HIV-positive subjects (Fig. 4 and Table 2). Because FACS sorting of HIV-infected cells requires paraformaldehyde fixation for biosafety reasons and paraformaldehyde can interfere with RNA isolation, DN as well as the CD4 + CD8 subset were isolated with magnetic beads. The cell yields for DN cells were on average 10-fold less than those for CD4 + CD8, consistent with percentages of DN cells ranging from 1.9% to 11.3% of total $CD3^+$ cells. As expected, the CD4 + CD8 subset contained 10- to 50-fold more RNA than the DN subsets, as assessed by cDNA titrations in an actin RT-PCR. However, RT-PCRs for MS RNA often yielded bands of similar intensity for DN versus CD4 + CD8, implying that the DN subset might be enriched for HIV MS RNA. Titrations for the MS RNA PCR (Fig. 4) confirmed this suggestion. For example, the ratio of endpoint dilutions (for the MS PCR, 1:40 or 0.025, and for the actin PCR, 1:40) are equivalent in patient c149. This equivalence suggests equal amounts of MS RNA in DN versus the CD4 + CD8 subset when normalized for total cellular RNA. In patient m122, the ratios suggest 16-fold enrichment of MS RNA in the DN subset. This result could be explained by higher percentages of productively infected cells in the DN subset, by more efficient viral transcription, or by a combination of both. Viral RNAs present in DN cells were not a rare finding. In 5 of 10 patients examined, US and/or MS RNA was detectable in the DN subset (Table 2). When HIV RNA was detectable in DN cells, it was also detectable in the CD4 + CD8 subset.

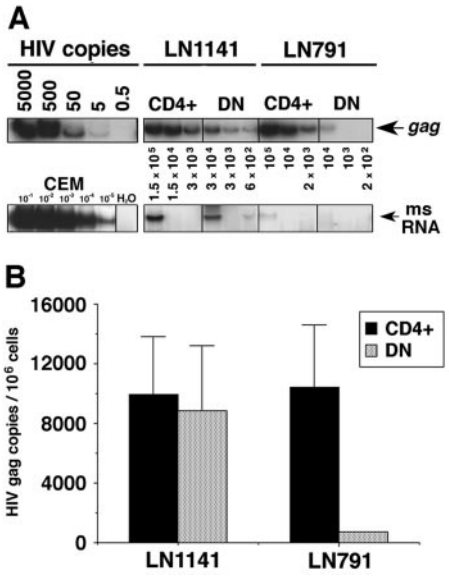

Fig. 3. HIV DNA in T cell subsets from LN. (*A*) *Gag* DNA PCR was performed on isolated CD4 and DN subsets from two LN. ACH-2 cell equivalents were used as an indicator of HIV-1 DNA copy numbers, and PCR substrate DNA from the LN subsets was diluted, as indicated by the cell number equivalents. cDNA templates were used for the MS RNA reverse transcription–PCR (RT-PCR) as described (7). The CEM cell line infected with HIV NL4.3 was used as a control for the specificity of the MS PCR with indicated dilutions starting at approximately 10^5 cell equivalents for the far left lane. (*B*) HIV *gag* DNA copy numbers per million cells were assessed as described for Fig. 2*B* by extrapolation on to a standard curve obtained from the ACH-2 dilutions. For each subset, three readings were taken by using the band intensities of the three dilutions, and these readings were used to calculate means ± SD.

HIV RNA in DN cells suggests productive HIV infection but does not prove that infectious virus is released. $CD4^+$, $CD8^+$, and $CD3^+$ DN cells were therefore isolated from HIV-positive subjects and cocultured with phytohemagglutinin-activated blasts that serve as indicators of viral transmission. Cell-free supernatants were assayed for p24 by ELISA at various time points as a measure of new HIV production (Fig. 5). HIV p24 was consistently detected from cocultures with $CD4^+$ and DN but not with $CD8^+$ or TN subsets. Virus produced by DN cells from CSS16.2 readily infected the indicator cells, resulting in p24 levels that were even higher than in the parallel culture with $CD4^+$ cells. Note that in patient CSS16, the preculture *gag* PCR band (Fig. 5 *Top Inset*) was much weaker for DN than for CD4 cells. For patient H1, HIV infection of the DN subset was not

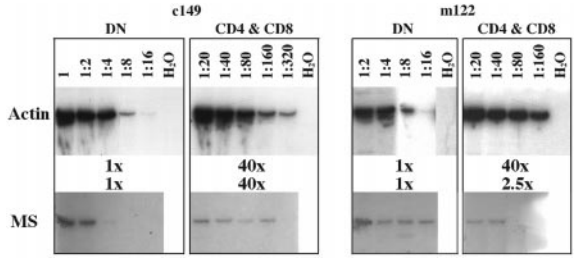

Fig. 4. Abundant HIV MS RNA in DN subset. DN as well as CD4 + CD8 subset isolated by magnetic beads from m122 and c149 were used to extract RNA and synthesize cDNA, which was quantitatively assessed by endpoint dilutions and comparisons with cellular actin cDNA. Congruent with the small percentages of DN cells per total $CD3^+$ cells in m122 and c149 (Table 2), actin RT-PCRs indicated an ≈40-fold excess of actin message in the CD4 + CD8 subset over the DN subset (arbitrarily assigned a 1× value). The ratios for MS RT-PCRs are compared with actin ratios to gauge relative excess of MS RNA in DN versus CD4 + CD8 subsets (see *Results*). For c149, the ratio is the same (1:40), indicating no enrichment of MS RNA in the DN subset; however, for m122, the ratio is 1:2.5 (16:40), representing a 16-fold enrichment of MS RNA in the DN subset.

Table 2. Viral RNA in T cell subsets

Patient	HIV per ml	CD4 per mm³	Subset	Actin	US	MS	No. cells ×10⁶	Percentage of DN cells per total CD3⁺ cells	Overnight culture	IL-2
ml40	3,000	413	DN	+	−	−	1.19	5.5		
			CD4 + CD8	+	−	−	20.30			
m38	60,251	93	DN	+	−	−	NA			
			CD4 + CD8	+	−	−	NA			
c145	462	233	DN	+	−	−	0.19	11.2	Y	Y
			CD4 + CD8	+	−	−	1.50		Y	Y
c150	<400	528	DN	+	−	−	2.59	11.3	Y	Y
			CD4 + CD8	+	−	−	20.3		Y	Y
c151	3,117	375	DN	+	−	−	0.13	9.8	Y	Y
			CD4 + CD8	+	−	−	1.19		Y	Y
m17	<400	340	DN	+	+	−	0.09	6.3	Y	Y
			CD4 + CD8	+	+	+	1.33		Y	Y
c146	<400	887	DN	+	+	+	0.19	4.9	Y	Y
			CD4 + CD8	+	−	+	3.70		Y	Y
c147	<400	373	DN	+	−	+	1.81	8.0	Y	
			CD4 + CD8	+	+	+	20.90		Y	
m122	<400	557	DN	+	+	−	0.57	1.9	Y	Y
			CD4 + CD8	+	+	−	30.1		Y	Y
			DN	+	−	+	0.57			
			CD4 + CD8	+	(+)	+	30.1			
c149	8,047	185	DN	+	+	+	0.94	5.9	Y	Y
			CD4 + CD8	+	+	+	15.0		Y	Y
			DN	+	(+)	+	0.94			
			CD4 + CD8	+	+	+	15.0			

The presence of detectable actin mRNA, HIV multispliced mRNA (MS), and HIV unspliced mRNA (US) in the subsets (see *Methods*; DN, $CD4^-$ $CD8^-$ $CD3^+$; CD4 + CD8) is indicated by +. (+) indicates that some experiments gave negative results. The cell numbers used to prepare the RNA from the isolated subset are indicated. The relative percentage of DN cells per total $CD3^+$ cells, clinical data on plasma viral load, and CD4 counts are also indicated. Some samples (indicated by Y) were cultured overnight in medium containing FCS with or without recombinant human IL-2. Each sample was analyzed at least twice.

even detectable before culture (Fig. 5 *Middle Inset*). However, infection of the indicator cells was readily seen when DN T cells of H1 were used as a source of virus. For patient Met70, DN T cells were also able to produce infectious virions, albeit with slower kinetics. In view of the much weaker DNA PCR signal in preculture DN cells versus preculture CD4 cells, DN cells infected with HIV were apparently able to produce infectious virus with greater efficiency. Finally, *gag* DNA was also measured by PCR in the infected indicator cells at the end of the cocultures (Fig. 5 *Insets*). HIV DNA was found in all three subsets (CSS16.2) or in $CD4^+$ and DN cells (H1) but not in the TN subset (data not shown), consistent with the p24 results. Although infectious HIV was rescued from the DN subset of three patients, rescue was not successful in samples from two other patients (CSS8 and Met90.3), both of which had undetectable plasma viral loads (data not shown).

Discussion

Down-regulation of CD4 from the cell surface has been well documented in transformed T cell lines infected in the laboratory (17) and in primary lymphocytes infected with a reporter virus (6, 7). If this down-regulation occurs *in vivo*, one would expect to find HIV-infected DN T cells as described in this study, the first comprehensive analysis of HIV infection in this subset. Although we can neither rule out direct infection of some DN T cells nor exclude that some HIV-positive DN cells derive from infected thymocytes, the simplest explanation for the presence of HIV-positive DN T cells *in vivo* is CD4 down-regulation occurring after infection of peripheral $CD4^+$ precursors. If HIV-positive DN cells are former $CD4^+$ cells, one would expect continued expression of CD4 mRNA, as previously shown in PBL, infected *in vitro* with a reporter virus (7). We tested for the presence of CD4 mRNA in CD4, CD8, and DN subsets sorted from HIV-positive patients and found only small amounts of CD4 mRNA in DN cells and in CD8 cells in both HIV-positive and HIV-negative subjects (data not shown). These results are compatible with a $CD4^+$ origin of HIV infected DN T cells. The absence of high levels of CD4 mRNA in DN cells could be caused by low percentages of HIV-positive cells within the DN subset making it difficult to see increased CD4 mRNA when examining the entire DN subset. The data are also compatible with HIV-positive DN cells derived from other sources, such as thymic DN cells or natural killer T cells with a DN phenotype.

Direct proof for CD4 down-regulation *in vivo* would require tracking the generation of DN cells from $CD4^+$ precursors. A recent study in monkeys with recombinant simian immunodeficiency virus encoding green fluorescent protein clearly showed that the majority of cells testing positive for green fluorescent protein were $CD3^+$ and that a fraction of them were $CD4^-$ (18). Although no quantitative analysis of this subset was made, these results support our data in humans and indicate that the source of HIV-positive DN T cells is most likely infected $CD4^+$ precursors.

The data presented (Fig. 5) suggest that DN T cells were enriched for productive virus compared with $CD4^+$ T cells. Productive infection leads to high cellular levels of viral proteins, and the peptide products of *nef*, *env*, and *vpu* have a requisite and cooperative effect on CD4 down-regulation (6). These viral proteins would not be present unless the cell were productively infected. Therefore, cells with down-modulated surface CD4 may represent the fraction of infected cells in which virus is being produced.

Given the redundancy of HIV genes that can mediate CD4 down-regulation, it is likely that this process is important for efficient viral replication. Viral replication in T cells is believed to result directly in cell death and eventual depletion of CD4 T cells (19). However, the paradigm of high CD4 cell turnover and destruction leading to CD4 depletion has been challenged (20) and the importance of T cell production in maintenance of the peripheral pool of naive cells is increasingly recognized (21). Others have

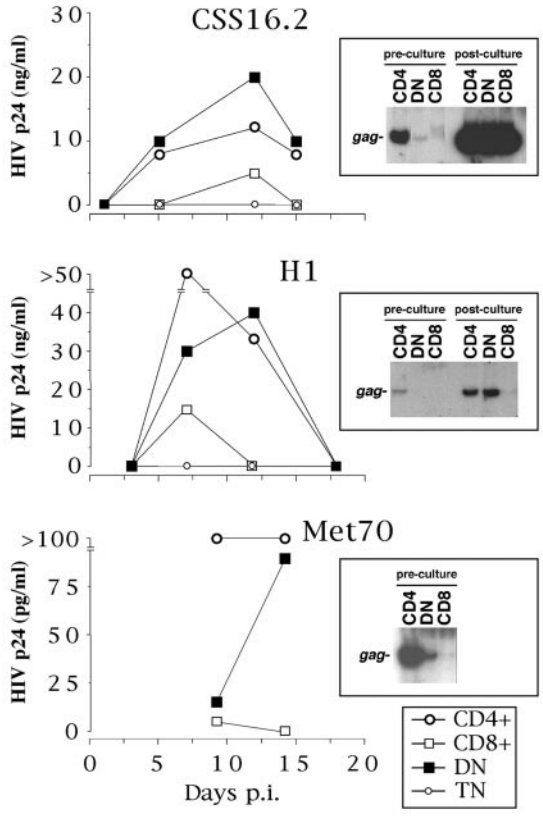

Fig. 5. Efficient production of infectious HIV from sorted DN subset. Different fractions of cells from HIV-positive patients were sorted with magnetic beads and cocultured with phytohemagglutinin-activated blasts. Cell-free supernatants were assayed for p24 by using an ELISA. DNA *gag* PCRs on preculture and postculture sorted subsets are shown in the *Insets*.

noted that apoptosis in *ex vivo* LN tissues is not correlated with the stage of the disease or viral burden (22) and that it rarely affects productively HIV-infected T cells, affecting instead the surrounding uninfected bystander T cells (23). These results point to indirect mechanisms of cell death that may contribute to overall $CD4^+$ depletion. Of these mechanisms, gp120-induced cell death has been the focus of several studies (4, 24, 25). One possibility is that CD4 down-regulation protects against apoptosis induced by cross-linking of CD4 by gp120. Indeed, we have shown that, in human PBL infected with a reporter virus (7), DN T cells are protected from gp120-induced apoptosis (G.M., unpublished data). It is therefore possible that CD4 down-regulation extends the half-life of productively infected T cells *in vivo* by rendering them less prone to gp120-induced apoptosis.

A major current obstacle in eradicating HIV from patients is the persistence of virus in quiescent T cells despite years of HAART. Quiescent $CD4^+$ T cells have been described as a major "reservoir" of replication-competent virus after initiation of HAART (26–29). These infected cells may have a long half-life *in vivo* (30) and are thought to be important in continued low-level viral production after initial viremia has abated and also in the reappearance of infectious virus after cessation of HAART. The DN T cells described herein are unlikely to represent quiescent T cells similar to the long-lived reservoir CD4 cells. Rather, we surmise that they represent the direct descendants of the quiescent cells, namely those producing infectious HIV. *In vitro* studies showed that the infected DN cells were observed exclusively after T cell activation and that they had a phenotype of activated memory T cells (7). We hypothesize that the same applies to infected DN cells *in vivo*.

Infected DN cells can be readily detected in patients on successful HAART in which the plasma viral load is undetectable. These infected DN cells represent evidence of continued HIV production in most patients even after a HAART response. HIV infection is rarely monitored by testing cellular viral loads. The reticence may be related to the presence of much abortive infection in CD4+ cells and therefore "dead" viral DNA. However, infected DN cells may be T cells that by definition contain live virus that is able to produce the viral proteins that down-modulate CD4.

The authors would like to thank all the subjects for their participation in this study, Dr. W. Telford for expert cell sorting, and Dr. A. Chadburn for the LN specimens. This work was supported in part by a fellowship from the Association pour la Recherche Contre le Cancer to G.M. and Public Health Service Grant RO-1 AI22333 (to D.N.P.).

1. Dalgleish, A. G., Beverly, P. C. L., Clapham, P. R., Crawford, D. H., Greaves, M. F. & Weiss, R. A. (1984) *Nature (London)* **312,** 763–767.
2. Klatzmann, D., Barre-Sinoussi, F., Nugeyre, M. T., Danquet, C., Vilmer, E., Griscelli, C., Brun-Veziret, F., Rouzioux, C., Gluckman, J. C., Chermann, J. C., et al. (1984) *Science* **225,** 59–63.
3. Aiken, C., Konner, J., Landau, N. R., Lenburg, M. E. & Trono, D. (1994) *Cell* **76,** 853–864.
4. Banda, N. K., Bernier, J., Kurahara, D. K., Kurrle, R., Haigwood, N., Sekaly, R.-P. & Finkel, T. H. (1992) *J. Exp. Med.* **176,** 1099–1106.
5. Benson, R. E., Sanfridson, A., Ottinger, J. S., Doyle, C. & Cullen, B. R. (1993) *J. Exp. Med.* **177,** 1561–1566.
6. Chen, B. K., Gandhi, R. T. & Baltimore, D. (1996) *J. Virol.* **70,** 6044–6053.
7. Marodon, G., Landau, N. R. & Posnett, D. N. (1999) *AIDS Res. Hum. Retroviruses* **15,** 161–171.
8. Yoshimoto, T., Bendelac, A., Watson, C., Hu-Li, J. & Paul, W. E. (1995) *Science* **270,** 1845–1847.
9. Psallidopoulos, M. C., Schnittman, S. M., Thompson, L. M., III, Baseler, M. & Fauci, A. S. (1989) *J. Virol.* **63,** 4626–4631.
10. Schnittman, S. M., Psallidopoulos, M. C., Lane, H. C., Thompson, L., Baseler, M., Massari, F., Fox, C. H., Salzman, N. P. & Fauci, A. S. (1989) *Science* **245,** 305–308.
11. Flamand, L., Crowley, R. W., Lusso, P., Colombini-Hatch, S., Margolis, D. M. & Gallo, R. C. (1998) *Proc. Natl. Acad. Sci. USA* **95,** 3111–3116.
12. Livingstone, W. J., Moore, M., Innes, D., Bell, J. E. & Simmonds, P. (1996) *Lancet* **348,** 649–654.
13. Ou, C. Y., Kwok, S., Mitchell, S. W., Mack, D. H., Sninsky, J. J., Krebs, J. W., Feorino, P., Warfield, D. & Schochetman, G. (1988) *Science* **239,** 295–297.
14. Dobrescu, D., Kabak, S., Mehta, K., Suh, C. H., Asch, A., Cameron, P. U., Hodtsev, A. S. & Posnett, D. N. (1995) *Proc. Natl. Acad. Sci. USA* **92,** 5563–5567.
15. Pantaleo, G., Graziosi, C., Demarest, J. F., Butini, L., Montroni, M., Fox, C. H., Orenstein, J. M., Kotler, D. P. & Fauci, A. S. (1993) *Nature (London)* **362,** 355–358.
16. Embretson, J., Zupancic, M., Ribas, J. L., Burke, A., Racz, P., Tenner-Racz, K. & Haase, A. T. (1993) *Nature (London)* **362,** 359–362.
17. Bour, S., Geleziunas, R. & Wainberg, M. A. (1995) *Microbiol. Rev.* **59,** 63–93.
18. Alexander, L., Veazey, R. S., Czajak, S., DeMaria, M., Rosenzweig, M., Lackner, A. A., Desrosiers, R. C. & Sasseville, V. G. (1999) *AIDS Res. Hum. Retroviruses* **15,** 11–21.
19. Gandhi, R. T., Chen, B. K., Straus, S. E., Dale, J. K., Lenardo, M. J. & Baltimore, D. (1998) *J. Exp. Med.* **187,** 1113–1122.
20. Wolthers, K. C., Schuitemaker, H. & Miedema, F. (1998) *Immunol. Today.* **19,** 44–48.
21. Hellerstein, M., Hanley, M. B., Cesar, D., Siler, S., Papageorgopoulos, C., Wieder, E., Schmidt, D., Hoh, R., Neese, R., Macallan, D., *et al*. (1999) *Nat. Med*. **5,** 83–89.
22. Muro-Cacho, C. A., Pantaleo, G. & Fauci, A. S. (1995) *J. Immunol* **154,** 5555–5566.
23. Finkel, T. H., Tudor-Williams, G., Banda, N. K., Cotton, M. F., Curiel, T., Monks, C., Baba, T. W., Ruprecht, R. M. & Kupfer, A. (1995) *Nat. Med.* **1,** 129–134.
24. Nardelli, B., Gonzalez, C. J., Schechter, M. & Valentine, F. T. (1995) *Proc. Natl. Acad. Sci. USA* **92,** 7312–7316.
25. Cottrez, F., Manca, F., Dalgleish, A. G., Arenzana-Seisdedos, F., Capron, A. & Groux, H. (1997) *J. Clin. Invest.* **99,** 257–266.
26. Finzi, D., Hermankova, M., Pierson, T., Carruth, L. M., Buck, C., Chaisson, R. E., Quinn, T. C., Chadwick, K., Margolick, J., Brookmeyer, R., *et al*. (1997) *Science* **278,** 1295–1300.
27. Chun, T. W., Stuyver, L., Mizell, S. B., Ehler, L. A., Mican, J. A., Baseler, M., Lloyd, A. L., Nowak, M. A. & Fauci, A. S. (1997) *Proc. Natl. Acad. Sci. USA* **94,** 13193–13197.
28. Chun, T.-W., Carruth, L., Finzi, D., Shen, X., DiGiuseppe, J. A., Taylor, H., Hermankova, M., Chadwich, K., Margolick, J., Quinn, T. C., *et al*. (1997) *Nature (London)* **387,** 183–188.
29. Wong, J. K., Hezareh, M., Gunthard, H. F., Havlir, D. V., Ignacio, C. C., Spina, C. A. & Richman, D. D. (1997) *Science* **278,** 1291–1295.
30. Ho, D. D. (1997) *J. Clin. Invest.* **99,** 2565–2567.